can be determined as a function of the pursuer and evader speeds, as stated in the following Lemma.

Lemma III.3: In order for DSS *to satisfy the requirements of eventual pursuit control stated in Theorem II.*1*, the duration of each transmission slot* s_w *must be smaller than* $(1/12\eta_s v_e)(1 - (\alpha + k + 1)/k\alpha)$.

As evader speed decreases, we note that the requirement on the network service is relaxed and the allowable slot width increases which consequently reduces the cost of communication. Thus we are able to select network parameters that minimally satisfy the conditions for successful pursuit control, enabling us to optimize overall system performance. A similar analysis can be performed with respect to adjusting the communication cost based on allowable rates and error, which for reasons of space have not been presented here.

IV. Conclusion

In this technical note, we adopted a co-design approach to operate a distributed control application on top of a wireless sensor network by exploiting distance sensitivity as a locality concept. The snapshot service designed in this technical note can be additionally optimized for efficiency in the following ways: 1) First compression in the temporal domain can be achieved by transmitting only the state of nodes that have changed from the previous *round*. 2) Secondly, with knowledge of future pursuer locations, the algorithm can be tuned at run-time to supply only aggregated information in specific directions and thereby realize savings in communication cost. In this technical note, we have ignored errors in the underlying object detection service with respect to object localization, track association, false alarms and missed detections. Consideration of these errors for reliable pursuit control is feasible and is an interesting avenue for further research.

References

[1] B. Sinopoli, C. Sharp, L. Schenato, S. Schaffert, and S. Sastry, "Distributed control applications within sensor networks," *Proc. IEEE*, vol. 91, no. 8, pp. 1235–46, Aug. 2003.

[2] H. Cao, E. Ertin, and A. Arora, "Minimax equilibrium of networked differential games," *ACM Trans. Autonom. Adaptive Syst.*, vol. 3, no. 4, pp. 1–21, 2008.

[3] M. Demirbas, A. Arora, and M. Gouda, "A pursuer-evader game for sensor networks," in *Proc. 6th Symp. Self-Stabilizing Syst. (SSS)*, 2003, pp. 1–16.

[4] J. Lewin and J. Breakwell, "The surveillance-evasion game of degree," *J. Optim. Theory Appl.*, vol. 16, no. 3-4, pp. 339–353, 1975.

[5] J. Breakwell and A. Merz, "Toward a complete solution of homicidal chauffeur problem," in *Proc. Int. Conf. Theory Appl. Differ. Games*, 1969, pp. III-1–III-5.

[6] T. Muppirala, R. Murrieta-Cid, and S. Hjutchinson, "Optimal motion strategies based on critical events to maintain visibility of a moving target," in *Proc. IEEE Int. Conf. Robot. Autom. (ICRA)*, Apr. 2005, pp. 3826–3831.

[7] P. Kachroo, S. A. Shedied, and H. Vanlandingham, "Pursuit evasion: The herding noncooperative dynamic game—The stochastic model," *IEEE Trans. Syst., Man, Cybern.*, vol. 32, no. 1, pp. 37–42, Feb. 2002.

[8] K. Fregene, D. C. Kennedy, and D. W. L. Wang, "Toward a systems and control-oriented agent framework," *IEEE Trans. Syst., Man, Cybern.*, vol. 35, no. 5, pp. 999–1012, Oct. 2005.

[9] R. Issacs, *Differential Games*. New York: Wiley, 1965.

[10] L. Schenato, S. Oh, and S. Sastry, "Swarm coordination for pursuit evasion games using sensor networks," in *Proc. Int. Conf. Robot. Autom.*, 2005, pp. 2493–2498.

[11] R. Vidal, O. Shakernia, H. J. Kim, D. H. Shim, and S. Sastry, "Probabilistic pursuit-vvasion games: Theory, implementation, and experimental evaluation," *IEEE Trans. Robot. Autom.*, vol. 18, no. 5, pp. 662–669, Oct. 2002.

[12] D. P. Spanos, R. Olfati-Saber, and R. M. Murray, "Approximate distributed kalman filtering in sensor networks with quantifiable performance," in *Proc. 4th Int. Symp. Inform. Processing Sensor Networks (IPSN)*, Piscataway, NJ, 2005, p. 18.

[13] M. Chandy and L. Lamport, "Distributed snapshots: Determining global states of distributed systems," *ACM Trans. Comp. Syst.*, vol. 3, no. 5, pp. 63–75, 1985.

[14] J. Shin, L. Guibas, and F. Zhao, "A distributed algorithm for managing multi-target indentities in wireless ad hoc networks," in *Proc. Int. Workshop Inform. Processing Sensor Networks IPSN*, 2003, pp. 223–238.

[15] V. Kulathumani, "Network Abstractions for Designing Reliable Applications Using Wireless Sensor Networks," Ph.D. dissertation, Ohio State Univ., Columbus, OH, 2008.

[16] M. Demirbas, A. Arora, V. Mittal, and V. Kulathumani, "A fault-local self-stabilizing clustering service for wireless *ad hoc* networks," *IEEE Trans. Parallel Distrib. Syst.*, vol. 17, no. 9, pp. 912–922, Sep. 2006.

[17] V. Mittal, M. Demirbas, and A. Arora, Loci: Local Clustering Service for Large Scale Wireless Sensor Networks The Ohio State University, Columbus, OH, Tech. Rep. OSU-CISRC-2/03-TR07, 2003.

Communication-Aware Motion Planning in Mobile Networks

Alireza Ghaffarkhah and Yasamin Mostofi

***Abstract*—In this technical note, we propose a communication-aware motion planning framework to increase the probability that a robot maintains its connectivity to a fixed station, while accomplishing a sensing task, in realistic communication environments. We use a probabilistic multi-scale model for channel characterization. Using this model, we propose a probabilistic framework for assessing the spatial variations of a wireless channel, based on a small number of measurements. We then show how our channel learning framework can be utilized for devising communication-aware motion planning strategies. We first present communication-aware objective functions that can plan the trajectory of the robot in order to improve its online channel assessment in an environment. We then propose a communication-aware target tracking approach for the case where a fixed station utilizes a robot (or a number of them) to keep track of the position of a moving target. In this approach, probabilistic channel assessment metrics are combined with sensing goals, when controlling the motion, in order to increase the amount of information that the fixed station receives about the target. Finally, we show the performance of our framework, using both real and simulated channel measurements. Overall, our results indicate that networked robotic operations can benefit considerably from our probabilistic channel assessment and its integration with sensing/motion planning.**

***Index Terms*—Communication-aware target tracking, mobile sensor networks, probabilistic channel learning.**

I. Introduction

Over the past few years, considerable progress has been made in the area of networked robotic and control systems. Several different aspects of such systems have been studied, such as multi-agent coordination and connectivity maintenance [3], [4].

Communication plays a key role in the overall performance of robotic networks as the nodes exchange information with their team-

Manuscript received March 28, 2010; revised April 26, 2011; accepted July 22, 2011. Date of publication August 08, 2011; date of current version October 05, 2011. This paper appeared in part in ACC'10 and ICRA'10. This work was supported in part by ARO CTA MAST Project W911NF-08-2-0004 and NSF Award 0812338. Recommended by Associate Editor I. Stojmenovic.

The authors are with the Department of Electrical and Computer Engineering, University of New Mexico, Albuquerque, NM 87113 USA (e-mail: alinem@ece.umn.edu; ymostofi@ece.unm.edu).

Color versions of one or more of the figures in this technical note are available online at http://ieeexplore.ieee.org.

Digital Object Identifier 10.1109/TAC.2011.2164033

mates and/or supervising units. Most current work on networked robotic systems, however, assume ideal or over-simplified communication link models since ensuring the robust and coordinated operation of a number of robots is already considerably challenging.

More recently, a number of papers have started to highlight the importance of considering realistic communication links in cooperative control scenarios [1], [2], [5]–[7]. For instance, Mostofi shows how to integrate path loss communication models with the motion planner of the robots, for a cooperative robotic operation [6]. Lindhe and Johansson consider a single robot, with a predefined trajectory, and propose a stop-and-go policy to increase the amount of received information at a remote base station, based on the online measurements of the received SNR [5]. In [6], Mostofi also shows the impact of both highly correlated and uncorrelated fading channels on a cooperative target tracking operation, when the motion planner uses ideal path loss models to characterize the links. The results indicate that simplified link models may not suffice for ensuring robust networked operation. This necessitates considering realistic link models and properly integrating them in the motion planning objective functions, which is the main motivation for the work presented in this technical note.

In this technical note, we are interested in networked target tracking in realistic communication environments that experience fading. More specifically, a fixed station utilizes a robot (or a number of them) for keeping track of the position of a moving target. The communication between the robot and the station, however, experiences distance-dependent path loss and fading. Thus, in order for the robot to devise communication-aware motion planning objective functions, proper modeling and assessment of link qualities is required. The main contribution of this technical note is then as follows. We first present a framework for the probabilistic assessment of wireless channels, based on a small number of measurements. In this framework, we 1) model the channel with its three main underlying dynamics, i.e., path loss, shadow fading and multipath fading, 2) show how to learn the underlying model parameters online and 3) show how to probabilistically assess the channel at unvisited positions, based on this model. Then, we show how to build communication-aware motion planning objective functions, using the channel assessment framework. In particular, we consider two cases. First, we show how a node can devise its motion planner in order to better assess the channel quality. Second, we show how online channel assessments can be properly combined with sensing and exploration goals, to design communication-aware motion planning objective functions. We emphasize that we are not suggesting that a wireless channel is fully predictable, as it is not. Thus, instead of trying to capture and learn all the underlying dynamics of the channel, our proposed framework is aimed at probabilistically assessing the channel. As a result, our assessment of channel spatial variations is not going to be perfect, unless several measurements are gathered, but will be informative for the communication-aware control of motion. Furthermore, while our framework can be extended to the case where a number of robots coordinate their explorations, in this technical note we do not consider coordination among the robots, in order to focus on devising communication-aware motion objective functions that can address connectivity issues to the fixed station in realistic fading environments.

The rest of the technical note is organized as follows. In Section II, we describe our system model and briefly summarize the probabilistic multi-scale modeling of a wireless channel. We then use this model and present a probabilistic channel assessment framework. In Section III, we use our channel assessment framework and propose communication-aware motion-planning objective functions for both channel learning and cooperative target tracking. We conclude in Section IV.

II. Probabilistic Assessment of the Spatial Variations of a Wireless Channel

Consider a robotic operation, in a workspace $\mathcal{W} \subset \mathbb{R}^2$, in which a node (or a number of them) needs to maintain its connectivity to a fixed station while accomplishing a sensing task. We refer to the fixed station as a base station in this technical note. A fundamental parameter that characterizes the performance of the communication channel from a node to the base station is the instantaneous channel power. In this section, we introduce a framework to probabilistically assess the channel power, at unvisited locations, based on a small number of channel power measurements. For more details on this framework and the impact of different environments on its performance, see [2] and [8].

In the wireless communication literature [9], it is well established that the channel power (or equivalently the received signal power) can be modeled as a multi-scale system with three major dynamics: *path loss*, *shadow fading (or shadowing)* and *multipath fading (or small-scale fading)*. Let $\Upsilon(q)$ denote the channel power in the transmission from a node at position $q \in \mathcal{W}$ to the base station. By using a 2-D non-stationary random field model, we have the following characterization for $\Upsilon(q)$ (in dB) : $\Upsilon_{\mathrm{dB}}(q) = K_{\mathrm{PL}} - 10 n_{\mathrm{PL}} \log_{10}\left(\|q - q_b\|\right) + \Upsilon_{\mathrm{SH}}(q) + \Upsilon_{\mathrm{MP}}(q)$, where $\Upsilon_{\mathrm{dB}}(q) = 10\log_{10}\left(\Upsilon(q)\right)$, q_b is the position of the base station and $\Upsilon_{\mathrm{SH}}(q)$ and $\Upsilon_{\mathrm{MP}}(q)$ are independent random variables, representing the effects of shadow fading and multipath fading in dB, respectively [9]. The multipath fading term, in this paper, denotes the impact of multipath fading after normalization in the linear domain and subtraction of its average in the dB domain [8]. The distance-dependent path loss has a linear decay in the dB domain. Then, K_{PL} and $-10 \times n_{\mathrm{PL}}$ represent its offset and slope, respectively. Next, we show how each mobile node can probabilistically assess the spatial variations of the channel power at unvisited locations, using a small number of channel measurements.[1] These measurements can be gathered by the node along its trajectory during the operation, gathered and communicated to it by other nodes (with similar receivers) operating in the same environment, or collected *a priori*. Note that predicting multipath fading, based on sparse spatially-distributed samples, is not feasible, due to its rapid variations. Thus, our channel prediction framework is based on assessing the path loss and shadowing components. For increasing robustness to multipath fading (and other modeling errors), see our proposed strategies in [10].

A. Probabilistic Channel Assessment Based on a Small Number of Channel Measurements

Let $\mathcal{Q}_{i,t} = \left\{q^i_{1,t}, \ldots, q^i_{\kappa_{i,t},t}\right\}$, for $\kappa_{i,t} = |\mathcal{Q}_{i,t}|$, denote the set of the positions corresponding to the small number of channel power measurements available to node i at time instant t. Assume that the receiver can estimate and remove the receiver thermal noise power from each reception, or that the receiver thermal noise power is negligible, as compared to the received signal power, such that a node can measure the received channel power with good accuracy. The stacked vector of the received channel power measurements (in dB), available to the ith node, can then be expressed by $Y_{i,t} = \Gamma_{i,t}\theta + \Xi_{i,t} + \Omega_{i,t}$, where $\Gamma_{i,t} = [\, 1_{\kappa_{i,t}} \quad -D_{i,t}\,]$, $1_{\kappa_{i,t}}$ denotes the $\kappa_{i,t}$-dimensional vector of all ones, $D_{i,t} = \left[10\log_{10}(\|q^i_{1,t} - q_b\|) \cdots 10\log_{10}(\|q^i_{\kappa_{i,t},t} - q_b\|)\right]^{\mathrm{T}}$,

[1] In what follows, we assume symmetric uplink and downlink channels, i.e., the channel from a node to the base station is taken identical to the one from the base station to the node. This is the case, for instance, if both transmissions occur in the same frequency band and are separated using Time Division Duplexing (TDD). If uplink and downlink use different frequency bands, then we assume that a few uplink channel measurements are sent back to the node, using a feedback channel, as is common in the communication literature [8]. These uplink measurements then form the basis of uplink channel assessment.

$\theta = [K_{\rm PL} \;\; n_{\rm PL}]^{\rm T}$, $\Xi_{i,t} = \left[\Upsilon_{\rm SH}(q^i_{1,t}) \cdots \Upsilon_{\rm SH}(q^i_{\kappa_{i,t},t})\right]^{\rm T}$ and $\Omega_{i,t} = \left[\Upsilon_{\rm MP}(q^i_{1,t}) \cdots \Upsilon_{\rm MP}(q^i_{\kappa_{i,t},t})\right]^{\rm T}$. Based on the commonly-used lognormal distribution for shadow fading and its reported exponential spatial correlation [9], $\Xi_{i,t}$ is a zero-mean Gaussian random vector with the covariance matrix $R_{i,t} \in \mathbb{R}^{\kappa_{i,t}\times\kappa_{i,t}}$, where $\left[R_{i,t}\right]_{\ell_1,\ell_2} = \xi^2 \exp\left(-\|q^i_{\ell_1,t} - q^i_{\ell_2,t}\|/\beta\right)$ for $1 \le \ell_1, \ell_2 \le \kappa_{i,t}$, with ξ^2 and β denoting the variance of the shadow fading component in dB and its *decorrelation distance*, respectively. As for multipath fading, distributions such as Rayleigh, Rician, Nakagami and lognormal are shown to match its probability density function (pdf) (in non-dB domain), depending on the environment [9], [11]. In this section, we assume lognormal multipath fading and a resulting Gaussian distribution for $\Omega_{i,t}$. Note that Rayleigh, Rician and Nakagami provide a better fit than lognormal in general. However, mathematical derivations of online channel assessment are easier with a lognormal distribution. This over-simplification is only for our modeling and assessment purposes. When we present our results in the subsequent sections, the multipath component of our simulated channels has a Nakagami distribution. We also take the elements of $\Omega_{i,t}$ to be uncorrelated due to the following reasons. First, there is no one good model that characterizes the correlation of multipath fading in all the environments since its correlation depends on the angle of arrival as well as receiver antenna pattern. Second, multipath component typically decorrelates very fast, making adaptation to its changes unfeasible. As a result, we take $\Omega_{i,t}$ to be a zero-mean Gaussian random vector with the covariance $\omega^2 I_{\kappa_{i,t}}$, where ω^2 is the power of multipath fading component (in dB) and $I_{\kappa_{i,t}}$ is the $\kappa_{i,t}$-dimensional identity matrix. The first step in our probabilistic channel assessment is to estimate the parameters of the underlying model (θ, ξ, β and ω), based on the available measurements. We have the following lemma:

Lemma 1: Define $\alpha \triangleq \xi^2 + \omega^2$. Then, the Least Square (LS) estimation of the channel parameters, at the ith node and at time t, are given as follows: $\hat{\theta}_{i,t} = (\Gamma^{\rm T}_{i,t}\Gamma_{i,t})^{-1}\Gamma^{\rm T}_{i,t}Y_{i,t}$, $\hat{\alpha}_{i,t} = (1/\kappa_{i,t})Y^{\rm T}_{i,t,c}Y_{i,t,c}$, $[\hat{\xi}^2_{i,t}, \hat{\beta}_{i,t}] = \arg\min_{\xi^2,\beta} \sum_{d\in\mathcal{L}_{i,t}} \tau(d)\left[\log(\xi^2 e^{-d/\beta}) - \log(\hat{r}_{i,t}(d))\right]^2$ and $\hat{\omega}^2_{i,t} = \hat{\alpha}_{i,t} - \hat{\xi}^2_{i,t}$, where $Y_{i,t,c} = \left(I_{\kappa_{i,t}} - \Gamma_{i,t}(\Gamma^{\rm T}_{i,t}\Gamma_{i,t})^{-1}\Gamma^{\rm T}_{i,t}\right)Y_{i,t}$ represents the centered version of the measurement vector, $\hat{r}_{i,t}(d) = (1/|\mathcal{S}_{i,t}(d)|)\sum_{(\ell_1,\ell_2)\in\mathcal{S}_{i,t}(d)} \left[Y_{i,t,c}\right]_{\ell_1}\left[Y_{i,t,c}\right]_{\ell_2}$ is the numerical estimate of the spatial correlation at distance d, with $\mathcal{S}_{i,t}(d) = \left\{(\ell_1,\ell_2) | q^i_{\ell_1,t}, q^i_{\ell_2,t} \in \mathcal{Q}_{i,t}, \|q^i_{\ell_1,t} - q^i_{\ell_2,t}\| = d\right\}$. Furthermore, $\tau(d)$ is an associated weight that can be chosen based on the assessment of the accuracy of the estimation of $\hat{r}_{i,t}(d)$ (for instance, based on the number of available samples at distance d) and $\mathcal{L}_{i,t} = \left\{d \middle| 0 < \hat{r}_{i,t}(d) < \hat{\alpha}_{i,t}\right\}$.

Proof: It is straightforward to confirm that $\hat{\theta}_{i,t}$ minimizes $\|Y_{i,t} - \Gamma_{i,t}\theta\|^2$. The estimate of α is then given as $(1/\kappa_{i,t})\left(Y_{i,t} - \Gamma_{i,t}\hat{\theta}_{i,t}\right)^{\rm T}\left(Y_{i,t} - \Gamma_{i,t}\hat{\theta}_{i,t}\right)$. The estimation of ξ and β is based on minimizing the square error between the log of the estimated spatial correlation and its exact value. Finally, given $\hat{\alpha}_{i,t}$ and $\hat{\xi}^2_{i,t}$, we have $\hat{\omega}^2_{i,t} = \hat{\alpha}_{i,t} - \hat{\xi}^2_{i,t}$.[2] ■

Once the underlying channel parameters are estimated, the ith node can probabilistically assess the channel power, at an unvisited location, as given by the following lemma:

[2]If the location of the fixed station is not known, path loss parameters can be estimated by finding the best line fit to the log of the received measurements. Then, α can be estimated by calculating the deviation from the estimated path loss curve, followed by estimating ξ, β and ω as described in Lemma 1. Alternatively, the location of the fixed station can also be added to the unknown parameters and jointly estimated.

Lemma 2: Based on the measurements available to the ith node at time t and conditioned on the channel parameters, a Gaussian distribution with mean $\hat{\Upsilon}_{{\rm dB},i,t}(q) = \mathbb{E}\left\{\Upsilon_{\rm dB}(q)\middle|Y_{i,t},\theta,\beta,\xi,\omega\right\}$ and variance $\sigma^2_{i,t}(q) = \mathbb{E}\left\{\left(\Upsilon_{\rm dB}(q) - \hat{\Upsilon}_{{\rm dB},i,t}(q)\right)^2\middle|Y_{i,t},\theta,\beta,\xi,\omega\right\}$ can best characterize the channel at an unvisited position $q \in \mathcal{W}\setminus\mathcal{Q}_{i,t}$. We then have $\hat{\Upsilon}_{{\rm dB},i,t}(q) = \gamma^{\rm T}(q)\theta + \phi^{\rm T}_{i,t}(q)U^{-1}_{i,t}\left(Y_{i,t} - \Gamma_{i,t}\theta\right)$ and $\sigma^2_{i,t}(q) = \xi^2 + \omega^2 - \phi^{\rm T}_{i,t}(q)U^{-1}_{i,t}\phi_{i,t}(q)$, where $\gamma(q) = \left[1 \;\; -10\log_{10}\left(\|q - q_b\|\right)\right]^{\rm T}$, $U_{i,t} = R_{i,t} + \omega^2 I_{\kappa_{i,t}}$ and $\phi_{i,t}(q) = \left[\xi^2 e^{-\|q-q^i_{1,t}\|/\beta} \cdots \xi^2 e^{-\|q-q^i_{\kappa_{i,t},t}\|/\beta}\right]^{\rm T}$.

Proof: Consider variables $z_1 \in \mathbb{R}^{d_1}$ and $z_2 \in \mathbb{R}^{d_2}$ that are jointly Gaussian, with mean vectors μ_{z_1} and μ_{z_2}, covariance matrices Σ_{z_1} and Σ_{z_2}, and cross covariance matrix Σ_{z_1,z_2}. Then the conditional distribution of z_1, given z_2, is Gaussian with mean vector $\mu_{z_1} + \Sigma_{z_1,z_2}\Sigma^{-1}_{z_2}(z_2 - \mu_{z_2})$ and covariance matrix $\Sigma_{z_1} - \Sigma_{z_1,z_2}\Sigma^{-1}_{z_2}\Sigma^{\rm T}_{z_1,z_2}$ [12]. Setting $z_1 = \Upsilon(q)$, for $q \in \mathcal{W}\setminus\mathcal{Q}_{i,t}$, and $z_2 = Y_{i,t}$ completes the proof. Note that $\hat{\Upsilon}_{{\rm dB},i,t}(q)$ represents the MMSE estimate of $\Upsilon_{\rm dB}(q)$. ■

Algorithm 1 summarizes the steps involved in our channel assessment framework. For a more comprehensive analysis of model learning and probabilistic channel assessment, as well as its performance using real channel measurements, readers are referred to [8]. Note that Lemma 2 assumes perfect parameter estimation. The ith node then substitutes its estimated channel parameters of Lemma 1 to calculate $\hat{\Upsilon}_{{\rm dB},i,t}(q)$ and $\sigma^2_{i,t}(q)$. In what follows, $\phi_{i,t,{\rm est}}(q)$, $U_{i,t,{\rm est}}$, $\hat{\Upsilon}_{{\rm dB},i,t,{\rm est}}(q)$ and $\sigma^2_{i,t,{\rm est}}(q)$ indicate the ith node's assessment of $\phi_{i,t}(q)$, $U_{i,t}$, $\hat{\Upsilon}_{{\rm dB},i,t}(q)$ and $\sigma^2_{i,t}(q)$, respectively, when the exact channel parameters are replaced by their estimated values. We next consider the impact of parameter estimation error on the performance of channel assessment.

Algorithm 1 Online Channel Assessment at the ith Node

1: Initialize $\mathcal{Q}_{i,0}$ using the available offline channel samples (if there is any);

2: **for all** $t \ge 1$ **do**

3: Update $\mathcal{Q}_{i,t}$ using the measurements gathered by the ith node (and any measurements received from others in the case of cooperative channel assessment);

4: Calculate the estimates $\hat{\theta}_{i,t}$, $\hat{\xi}_{i,t}$, $\hat{\beta}_{i,t}$ and $\hat{\omega}_{i,t}$, using Lemma 1;

5: Calculate the MMSE estimate $\hat{\Upsilon}_{{\rm dB},i,t,{\rm est}}(q)$ and its corresponding variance $\sigma^2_{i,t,{\rm est}}(q)$ for $q \in \mathcal{W}\setminus\mathcal{Q}_{i,t}$, using Lemma 2 and the estimated channel parameters of the previous step;

6: **end for**

B. *Sensitivity of Channel Assessment to Modeling Parameter Estimation Errors*

In this section, we explore the impact of modeling parameter errors on the overall channel assessment performance. Assume that estimated parameters are used for the MMSE estimation of the channel in Lemma 2. For any $q \in \mathcal{W}\setminus\mathcal{Q}_{i,t}$, we have $\Upsilon_{\rm dB}(q) - \hat{\Upsilon}_{{\rm dB},i,t,{\rm est}}(q) = \gamma^{\rm T}(q)\delta\theta_{i,t} + \Upsilon_{\rm SH}(q) + \Upsilon_{\rm MP}(q) - \phi^{\rm T}_{i,t,{\rm est}}(q)U^{-1}_{i,t,{\rm est}}\Gamma_{i,t}\delta\theta_{i,t} - \phi^{\rm T}_{i,t,{\rm est}}(q)U^{-1}_{i,t,{\rm est}}\left(\Xi_{i,t} + \Omega_{i,t}\right)$, where $\delta\theta_{i,t} = \theta - \hat{\theta}_{i,t}$. Let us define $\Delta^2_{i,t}(q) \triangleq \mathbb{E}\Big\{\Big(\Upsilon_{\rm dB}(q) -$

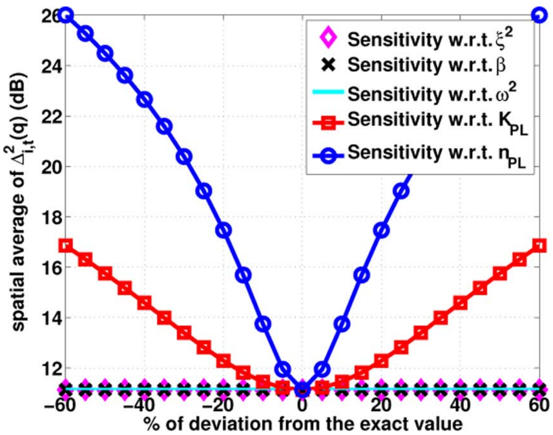

Fig. 1. Spatial average of $\Delta^2_{i,t}(q)$, as a function of the % of estimation error in $\hat{\theta}_{i,t}$, $\hat{\xi}^2_{i,t}$, $\hat{\beta}_{i,t}$ and $\hat{\omega}_{i,t}$.

$\hat{\Upsilon}_{\mathrm{dB},i,t,\mathrm{est}}(q)\Big)^2 \Big| Y_{i,t},\theta,\xi,\beta,\omega,\hat{\theta}_{i,t},\hat{\xi}_{i,t},\hat{\beta}_{i,t},\hat{\omega}_{i,t}\Big\}$. By conditioning on both the estimated and real parameters and using the fact that $\mathbb{E}\Big\{\Big(\Upsilon_{\mathrm{SH}}(q)+\Upsilon_{\mathrm{MP}}(q)\Big)\Big(\Xi_{i,t}+\Omega_{i,t}\Big)\Big\} = \phi_{i,t}(q)$, $\mathbb{E}\Big\{\Big(\Xi_{i,t}+\Omega_{i,t}\Big)\Big(\Xi_{i,t}+\Omega_{i,t}\Big)^{\mathrm{T}}\Big\} = U_{i,t}$ and $\mathbb{E}\Big\{\Big(\Upsilon_{\mathrm{SH}}(q)+\Upsilon_{\mathrm{MP}}(q)\Big)^2\Big\} = \xi^2+\omega^2$, we obtain: $\Delta^2_{i,t}(q) = \xi^2+\omega^2 - \phi^{\mathrm{T}}_{i,t,\mathrm{est}}(q)U^{-1}_{i,t,\mathrm{est}}\Big[2\phi_{i,t}(q) - U_{i,t}U^{-1}_{i,t,\mathrm{est}}\phi_{i,t,\mathrm{est}}(q)\Big] + \Big[\gamma(q) - \Gamma^{\mathrm{T}}_{i,t}U^{-1}_{i,t,\mathrm{est}}\phi_{i,t,\mathrm{est}}(q)\Big]^{\mathrm{T}}\delta\theta_{i,t}\delta\theta^{\mathrm{T}}_{i,t}\Big[\gamma(q) - \Gamma^{\mathrm{T}}_{i,t}U^{-1}_{i,t,\mathrm{est}}\phi_{i,t,\mathrm{est}}(q)\Big]$. Then, we have the following important question: which parameters have the most impact on channel assessment? While we leave the proof of this to our future work, we observed, from several channel assessments, that the channel assessment framework is most sensitive to the error in path loss estimation (mainly the slope error), which is also intuitive. Fig. 1 shows the impact of parameter estimation uncertainty on the overall channel assessment quality, where the spatial average of $\Delta^2_{i,t}(q)$, i.e., $\int_{\mathcal{W}}\Delta^2_{i,t}(q)\mathrm{d}q/\int_{\mathcal{W}}\mathrm{d}q$, is plotted for an indoor channel with the following parameters: $\theta = [-10 \quad 2.0]^{\mathrm{T}}$, $\xi = 2.0$ dB, $\beta = 1.0$ m and $\omega = 2.78$ dB (corresponding to a Nakagami distribution with parameter $m = 3.27$ [9]). The number of available channel measurements is 0.1% of the total samples (102 measurements for a 320×320 grid), with the measurements randomly distributed over the workspace. For each curve, only one parameter is perturbed while the rest are assumed perfect. It can be seen that channel assessment is considerably more sensitive to path loss parameters (especially the path loss exponent n_{PL}). As such, it becomes important to estimate the path loss parameters as accurately as possible. In Section III, we show how to do so by designing a proper motion planning objective function that is aimed at improving the estimation of path loss parameters.

III. Communication-Aware Motion Planning

The main purpose of communication-aware motion planning is to utilize the acquired knowledge on the link quality in order to properly plan the motion, in the presence of communication constraints. In this section, we propose communication-aware motion planning strategies for 1) better channel assessment and 2) task accomplishment of networked target tracking.

A. *Communication-Aware Motion Planning for Improving Wireless Channel Assessment*

Consider the case that a node is assessing the spatial variations of the channel to a fixed station, as discussed in the previous section. Since the node samples the channel along its trajectory, its motion directly impacts its channel assessment quality. Then, we want to answer the following question: *How should a node plan its trajectory in order to improve its channel assessment quality?* We first show how a node can plan its trajectory in order to improve its assessment of the underlying model parameters. This is then followed by planning the motion in order to decrease the channel estimation error variance. Note that in case a number of nodes are cooperating to better assess the channel, the framework here should be extended to include coordination among the nodes so that they avoid visiting the same area.

1) Motion Planning for Better Learning of the Underlying Model Parameters: Our model for the spatial variations of the channel depends on the parameters θ, ξ, β and ω. While the trajectory of a robot can be optimized to improve the estimation quality of all these parameters, we saw in Section II-B that channel estimation is considerably more sensitive to the accuracy of the estimation of θ, as compared to the rest of the parameters. Therefore, in this part we devise a motion planning strategy that aims at improving the quality of the estimation of θ, assuming that the estimation error of the rest of the parameters is negligible. Consider the case where $\kappa_{i,t} \geq 0$ channel measurements are available to the ith node at time instant t. Then, the node needs to plan its trajectory such that the next channel measurement it gathers, optimally improves its estimation of θ, as is characterized by the next lemma. We consider the more challenging case of Maximum Likelihood (ML) estimation of path loss parameters in the next lemma. A simpler result can be derived for the case of LS estimation.

Lemma 3: Assume negligible error in the estimation of ξ, β and ω. Let $\mathcal{M}_{\mathrm{ML},i,t}$ denote the error covariance of the ML estimation of the path loss parameters at the ith node and at time t, conditioned on shadowing and multipath parameters. Assume that the ith node gathers one more channel power measurement along its trajectory at time $t+1$. Then we have the following recursion for $\mathcal{M}_{\mathrm{ML},i,t}$:

$$\mathcal{M}^{-1}_{\mathrm{ML},i,t+1} = \mathcal{M}^{-1}_{\mathrm{ML},i,t} + \frac{\varphi_{i,t}(q_{i,t+1})\varphi^{\mathrm{T}}_{i,t}(q_{i,t+1})}{\sigma^2_{i,t}(q_{i,t+1})} \tag{1}$$

where $\varphi_{i,t}(q) \triangleq \gamma(q) - \Gamma^{\mathrm{T}}_{i,t}U^{-1}_{i,t}\phi_{i,t}(q)$ and $q_{i,t+1}$ is the position of the ith node at time $t+1$.

Proof: Based on the probabilistic modeling of the previous section, the ML estimation of θ and its corresponding estimation error covariance, using the channel power measurements up to time $t+1$ and conditioned on ξ, β and ω, are given by $\hat{\theta}_{\mathrm{ML},i,t+1} = \Big(\Gamma^{\mathrm{T}}_{i,t+1}U^{-1}_{i,t+1}\Gamma_{i,t+1}\Big)^{-1}\Gamma^{\mathrm{T}}_{i,t+1}U^{-1}_{i,t+1}Y_{i,t+1}$ and $\mathcal{M}_{\mathrm{ML},i,t+1} = \Big(\Gamma^{\mathrm{T}}_{i,t+1}U^{-1}_{i,t+1}\Gamma_{i,t+1}\Big)^{-1}$, where $U_{i,t+1} = \begin{bmatrix} \xi^2+\omega^2 & \phi^{\mathrm{T}}_{i,t}(q_{i,t+1}) \\ \phi_{i,t}(q_{i,t+1}) & U_{i,t}\end{bmatrix}$, $\Gamma_{i,t+1} = \Big[\gamma(q_{i,t+1}) \quad \Gamma^{\mathrm{T}}_{i,t}\Big]^{\mathrm{T}}$ and $q_{i,t+1} \notin \mathcal{Q}_{i,t}$. By using matrix inversion lemma for $U^{-1}_{i,t+1}$ and after some straightforward derivations, (1) is obtained. ■

Then, in order to minimize the estimation error covariance of θ in the next step, the ith node needs to maximize the second term on the right hand side of (1). Consider the following discrete dynamical model for the ith node: $q_{i,t+1} = \Psi_i(q_{i,t}, v_{i,t})$, where $v_{i,t} \in \mathcal{V}_i$ is the control input at time t, $\mathcal{V}_i$ is the set of admissible control inputs and $\Psi_i(\cdot,\cdot)$ is a known function. We then have the following next-step

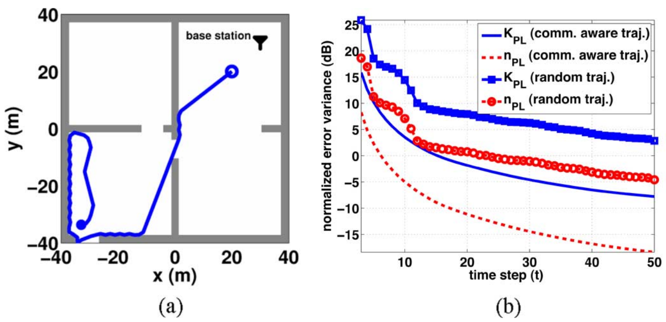

Fig. 2. (a) Trajectory of a mobile node in communication-aware motion planning for improving path loss parameter estimation in an indoor environment and (b) the corresponding normalized estimation error variance. The empty circle and the filled one in (a) denote the initial and final positions of the node.

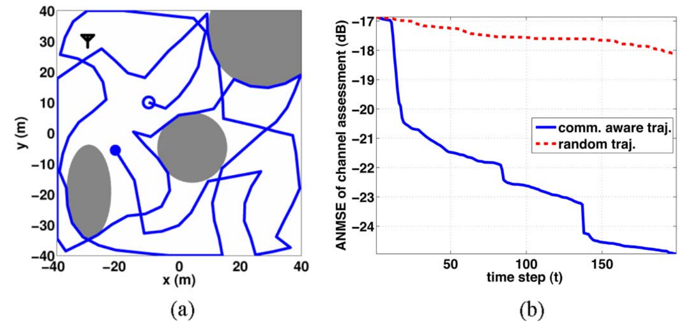

Fig. 3. (a) Trajectory of a mobile node in communication-aware motion planning for reducing channel assessment uncertainty in an outdoor environment and (b) the corresponding ANMSE. The empty circle and the filled one in (a) denote the initial and final positions of the node.

motion optimization problem, considering the trace of the right hand side of (1):

$$\begin{aligned} v_{i,t}^* &= \arg\max_{v_{i,t}} J_{\mathrm{PL},i,t}(q_{i,t+1}) \triangleq \frac{\left\|\varphi_{i,t,\mathrm{est}}(q_{i,t+1})\right\|^2}{\sigma_{i,t,\mathrm{est}}^2(q_{i,t+1})} \\ \text{s.t. } &1)\ q_{i,t+1} = \Psi_i\Big(q_{i,t}, v_{i,t}\Big), \\ &2)\ v_{i,t} \in \mathcal{V}_i, \\ &3)\ q_{i,t+1} \in \mathcal{W} \setminus \mathcal{O}_{i,t} \end{aligned} \tag{2}$$

where $\varphi_{i,t,\mathrm{est}}(q) = \gamma(q) - \Gamma_{i,t}^{\mathrm{T}} U_{i,t,\mathrm{est}}^{-1} \phi_{i,t,\mathrm{est}}(q)$ and $\phi_{i,t,\mathrm{est}}(q)$, $U_{i,t,\mathrm{est}}$ and $\sigma_{i,t,\mathrm{est}}^2(q)$ are the estimates of $\phi_{i,t}(q)$, $U_{i,t}$ and $\sigma_{i,t}^2(q)$, with the shadowing and multipath parameters replaced by their estimated values. Also, $\mathcal{O}_{i,t}$ denotes the set of forbidden areas (estimated by the ith node at time t) for obstacle/collision avoidance.

Fig. 2 shows the performance of the motion planner of (2) in an indoor environment that has obstacles (denoted by gray areas). The node starts with no *a priori* channel measurement in this environment. It then solves for its next position by locally optimizing (2) in a small area around its current position. In this example, the dynamical model of the node is given by $q_{t+1} = q_t + v_t$, where $\|v_t\| \leq 1.75$ (1.75 is the radius of the local search area in this case). The left and right figures show the trajectory of the node and its normalized path loss estimation error variance, respectively. The indoor channel is simulated with the same parameters of Fig. 1. The right figure also compares the performance with the case where the robot has a random trajectory (the random case is averaged over 50 runs). It can be seen that we gain considerably (around 10 dB) by using the optimization framework of (2).

2) Motion Planning for Reducing the Uncertainty of Channel Assessment: Once the parameters of the underlying model are estimated, the robot can plan its trajectory in order to reduce its channel assessment uncertainty. As characterized in Lemma 2, the estimation error variance of the channel assessment is as follows: $\sigma_{i,t}^2(q) = \xi^2 + \omega^2 - \phi_{i,t}^{\mathrm{T}}(q) U_{i,t}^{-1} \phi_{i,t}(q)$, for any $q \in \mathcal{W} \setminus \mathcal{Q}_{i,t}$ and assuming negligible error in the underlying parameters. Consider the case where a number of channel measurements are available to the ith node at time instant t. Then, the node can plan its motion to go towards the location with the highest channel assessment uncertainty, i.e., the largest $\sigma_{i,t}^2(q)$, based on the available measurements.[3] Define the following objective function: $J_{\mathrm{CH},i,t}(q) \triangleq \max\Big\{0, \sigma_{i,t,\mathrm{est}}^2(q) - \sigma_{\mathrm{TH}}^2\Big\}\psi\Big(\|q - q_{i,t}\|\Big)$, where $\sigma_{i,t,\mathrm{est}}^2(q)$ is the estimate of $\sigma_{i,t}^2(q)$, with the exact parameters replaced by the estimated ones, σ_{TH}^2 is a fixed threshold and $\psi(\cdot)$ is a non-increasing function of its argument. By thresholding $\sigma_{i,t,\mathrm{est}}^2(q)$, we remove the positions with negligible channel assessment uncertainty. Then, $\psi\Big(\|q - q_{i,t}\|\Big)$ weighs the remaining space based on closeness to the current position, favoring less movement. Let $q_{i,t}^* = \arg\max_{q \in \mathcal{W} \setminus \mathcal{Q}_{i,t} \cup \mathcal{O}_{i,t}} J_{\mathrm{CH},i,t}(q)$ denote the maximizing argument of $J_{\mathrm{CH},i,t}(q)$ over the workspace. $q_{i,t}^*$ is an obstacle/collision free position with high channel assessment uncertainty, that is also close to the current position. If motion cost is not an issue, ψ can be chosen one. In our results, we take $\psi(d) = e^{-\zeta d}$, for $\zeta \geq 0$. The motion of the ith node at time t (the corresponding control input) is then the solution of the following optimization problem:

$$\begin{aligned} v_{i,t}^* &= \arg\min_{v_{i,t}} \Big\|q_{i,t+1} - q_{i,t}^*\Big\|, q_{i,t}^* = \arg\max_{q \in \mathcal{W} \setminus \mathcal{Q}_{i,t} \cup \mathcal{O}_{i,t}} J_{\mathrm{CH},i,t}(q) \\ \text{s.t. } &1)\ q_{i,t+1} = \Psi_i\Big(q_{i,t}, v_{i,t}\Big), \\ &2)\ v_{i,t} \in \mathcal{V}_i, \\ &3)\ q_{i,t+1} \in \mathcal{W} \setminus \mathcal{O}_{i,t} \end{aligned} \tag{3}$$

where the rest of the parameters are the same as in (2).

Fig. 3 shows the performance of this motion planning approach for a single node in an outdoor environment with obstacles (denoted by gray areas), assuming negligible error in the estimation of the modeling parameters. The dynamical model of the node is given by $q_{t+1} = q_t + v_t$, where $\|v_t\| \leq 5.5$. The outdoor channel is simulated with the following parameters: $\theta = [-10 \quad 2]$, $\xi = 4$ dB, $\beta = 10.0$ m, $\omega = 1.99$ dB (for a Nakagami distribution with $m = 5.76$). Furthermore, $\sigma_{\mathrm{TH}}^2 = 4$ and $\zeta = 0.02$. The node starts with 0.016% *a priori* channel measurements, randomly chosen in the space (0.016% of the total number of workspace samples, i.e., 16 measurements for a 320×320 grid). Fig. 3(a) and (b) show the trajectory of the node and the time evolution of ANMSE, i.e., $(\int_{\mathcal{W} \setminus \mathcal{O}_{i,t}} (\Upsilon_{\mathrm{dB}}(q) - \hat{\Upsilon}_{\mathrm{dB},i,t,\mathrm{est}}(q))^2 / \Upsilon_{\mathrm{dB}}^2(q) \mathrm{d}q) / \int_{\mathcal{W} \setminus \mathcal{O}_{i,t}} \mathrm{d}q$, respectively. For the sake of comparison, the right figure also compares the performance with the case where the robot has a random trajectory (the random case is averaged over 50 runs). It can be seen that channel assessment uncertainty reduces considerably as the node intelligently plans its motion (for instance, at $t = 100$, the ANMSE is -22.62 dB, corresponding to the RMS error of 2.49).

B. Communication-Aware Target Tracking

Consider the case where a fixed base station utilizes N robots for keeping track of a position of a moving target. The overall goal is for

[3] Alternatively, the node can plan its motion in order to minimize the spatial average of channel assessment uncertainty over the workspace of interest [1]. We skip the details of this approach due to space limitations.

the station to constantly have a good assessment of the target position. In this section, we show how each node can utilize the probabilistic channel assessment framework of the previous section to devise a communication-aware motion planning objective function that increases the probability of its connectivity to the base station while accomplishing its target tracking task.[4]

The communication links between the robots and the base station experience path loss, shadow fading and multipath fading. We assume a packet-dropping receiver [1], [7] at the base station, i.e., the base station drops all the packets with the received channel power below a predefined threshold.[5] Let $\Upsilon_{\mathrm{dB,TH}}$ denote the equivalent channel power threshold. Then the received packet from the ith node is dropped, at time t, if $\Upsilon_{\mathrm{dB}}(q_{i,t}) < \Upsilon_{\mathrm{dB,TH}}$ and is kept otherwise. Let $p_t \in \mathbb{R}^2$ and $\dot{p}_t \in \mathbb{R}^2$ denote the position and velocity of the target, respectively, at time t, with $x_t = [p_t^{\mathrm{T}}\, \dot{p}_t^{\mathrm{T}}]^{\mathrm{T}}$. We consider the following dynamical model for the moving target [14]: $x_{t+1} = Ax_t + B\varsigma_t$, where $A = \begin{bmatrix} I_2 & \epsilon I_2 \\ 0 & I_2 \end{bmatrix}$, $B = \begin{bmatrix} (1/2)\epsilon^2 I_2 \\ \epsilon I_2 \end{bmatrix}$, ϵ is the discretization time step, $\varsigma_t \in \mathbb{R}^2$ is a zero-mean Gaussian noise with $\Theta = \mathbb{E}\left\{\varsigma_t \varsigma_t^{\mathrm{T}}\right\}$ representing its covariance matrix and I_2 is the 2×2 identity matrix. Let $z_{i,t} \in \mathbb{R}^2$ represent the measurement of the ith mobile node of x_t. We have $z_{i,t} = Hx_t + \vartheta_{i,t}$, where $H = [I_2 \quad 0]$ and $\vartheta_{i,t} \in \mathbb{R}^2$ is a zero-mean Gaussian observation noise with $\Lambda_{i,t} = \mathbb{E}\left\{\vartheta_{i,t}\vartheta_{i,t}^{\mathrm{T}}\right\}$ representing its covariance. $\Lambda_{i,t}$ depends on the positions of both the robot and the target [1], [14]: $\Lambda_{i,t} = \Phi\left(q_{i,t}, p_t\right)$, where $\Phi(\cdot,\cdot)$ is assumed known.

The remote base station constantly estimates the position of the target, based on the received observations and by using a Kalman filter. Let $\hat{x}_{t_1|t_2}$ represent the estimate of x_{t_1} at the base station, using all the received observations up to and including time t_2. Let $P_{t_1|t_2}$ denote the corresponding estimation error covariance, at the base station, given $\Upsilon_{\mathrm{dB}}(q_{i,0}), \ldots, \Upsilon_{\mathrm{dB}}(q_{i,t_2})$ for $t_2 \leq t_1$ and $i = 1, \ldots, N$. Also define $\mathcal{J}_{t_1|t_2} \triangleq \left(P_{t_1|t_2}\right)^{-1}$ (Fisher information matrix), $\chi_{t_1|t_2} \triangleq \mathcal{J}_{t_1|t_2}\hat{x}_{t_1|t_2}$ (information vector) and $\lambda_{i,t} \triangleq \begin{cases} 1 & \Upsilon_{\mathrm{dB}}(q_{i,t}) \geq \Upsilon_{\mathrm{dB,TH}} \\ 0 & \text{else} \end{cases}$. Then, assuming i.i.d. observation noises, the recursion for $\chi_{t|t}$ and $\mathcal{J}_{t|t}$ is given as follows: $\chi_{t+1|t+1} = \chi_{t+1|t} + \sum_{i=1}^{N} \lambda_{i,t+1} H^{\mathrm{T}} \Lambda_{i,t+1}^{-1} z_{i,t+1}$ and $\mathcal{J}_{t+1|t+1} = \mathcal{J}_{t+1|t} + \sum_{i=1}^{N} \lambda_{i,t+1} H^{\mathrm{T}} \Lambda_{i,t+1}^{-1} H$, where $\chi_{t+1|t} = \mathcal{J}_{t+1|t} A \mathcal{J}_{t|t}^{-1} \chi_{t|t}$ and $\mathcal{J}_{t+1|t} = \left(A\mathcal{J}_{t|t}^{-1}A^{\mathrm{T}} + B\Theta B^{\mathrm{T}}\right)^{-1}$. Let us define $\mathcal{I}_{i,t+1} \triangleq \lambda_{i,t+1} H^{\mathrm{T}} \Lambda_{i,t+1}^{-1} H$. As can be seen, $\mathcal{I}_{i,t+1}$ depends on both the sensing quality of the ith node as well as its communication quality to the base station. Since our assessment of the link qualities is probabilistic, $\mathcal{I}_{i,t+1}$ becomes stochastic due to its dependency on the link qualities. By averaging over channel distributions, we have $\mathbb{E}\left\{\mathcal{J}_{t+1|t+1}\right\} = \mathbb{E}\left\{\mathcal{J}_{t+1|t}\right\} + \sum_{i=1}^{N} \mathbb{E}\left\{\mathcal{I}_{i,t+1}\right\}$, with $\mathbb{E}\left\{\mathcal{I}_{i,t+1}\right\} = \mathrm{Prob}\left\{\Upsilon_{\mathrm{dB}}\left(q_{i,t+1}\right) \geq \Upsilon_{\mathrm{dB,TH}}\right\} H^{\mathrm{T}} \Lambda_{i,t+1}^{-1} H$, where $\mathrm{Prob}\left\{\Upsilon_{\mathrm{dB}}\left(q_{i,t+1}\right) \geq \Upsilon_{\mathrm{dB,TH}}\right\}$ is the probability that the received packet from the ith node is kept at the base station at time $t+1$. Then, the next step average Fisher information at the base station is maximized if node i maximizes its assessment of $\mathbb{E}\left\{\mathcal{I}_{i,t+1}\right\}$. The ith mobile node can estimate $\mathrm{Prob}\left\{\Upsilon_{\mathrm{dB}}\left(q_{i,t+1}\right) \geq \Upsilon_{\mathrm{dB,TH}}\right\}$, by using the channel assessment framework of the previous section, as follows: $\mathrm{Prob}\{\Upsilon_{\mathrm{dB}}(q_{i,t+1}) \geq \Upsilon_{\mathrm{dB,\,TH}}\} = Q\left((\Upsilon_{\mathrm{dB,TH}} - \Upsilon_{\mathrm{dB},i,t,\mathrm{est}}(q_{i,t+1}))/\sigma_{i,t,\mathrm{est}}(q_{i,t+1})\right)$, where $Q(a) = (1/\sqrt{2\pi})\int_a^{\infty} e^{-s^2/2} ds$ and $\Upsilon_{\mathrm{dB},i,t,\mathrm{est}}(q)$ and $\sigma_{i,t,\mathrm{est}}(q)$ are the estimates of $\Upsilon_{\mathrm{dB},i,t}(q)$ and $\sigma_{i,t}(q)$, respectively (see Lemma 2), with the exact parameters replaced by the estimated ones. Define the following motion objective function for the ith node, by considering the trace of the information matrix: $J_{\mathrm{TRCK},i,t}(q_{i,t+1}) \triangleq Q\left((\Upsilon_{\mathrm{dB,TH}} - \Upsilon_{\mathrm{dB},i,t,\mathrm{est}}(q_{i,t+1}))/\sigma_{i,t,\mathrm{est}}(q_{i,t+1})\right) \mathrm{tr}\left\{\Phi^{-1}(q_{i,t+1}, \hat{p}_{i,t+1|t})\right\}$. The time-varying $\hat{p}_{i,t+1|t}$ denotes the prediction of the ith node of the target position at time $t+1$, which it can assess by using a local Kalman filter. The control input of the ith node at time t, is then given by the following optimization problem:

$$\begin{aligned} v_{i,t}^{*} &= \arg\max_{v_{i,t}} J_{\mathrm{TRCK},i,t}(q_{i,t+1}) \\ \text{s.t. } &1)\ q_{i,t+1} = \Psi_i\left(q_{i,t}, v_{i,t}\right), \\ &2)\ v_{i,t} \in \mathcal{V}_i, \\ &3)\ q_{i,t+1} \in \mathcal{W} \setminus \mathcal{O}_{i,t}. \end{aligned} \quad (4)$$

Note that by using the trace of Fisher information, the overall next step information maximization at the base station decouples into maximizing N localized objective functions at individual nodes. In case other metrics are used (e.g., $\det(\cdot)$ or $\|\cdot\|$), the objective function may not be decentralizable, requiring coordination among the nodes. The objective function of (4) shows how channel learning is integrated with sensing objectives in order to ensure communication-aware operation. A node can start with *a priori* channel measurements in the environment, for channel assessment, or it can jointly assess the channel and track the target. The more channel measurements it gathers during the operation, the better it can evaluate the objective function of (4).

Fig. 4 shows a target tracking scenario in an outdoor environment that contains obstacles (gray areas), using three mobile nodes. We use mobile agents with the following dynamics: $q_{i,t+1} = q_{i,t} + v_{i,t}$ for $\|v_{i,t}\| \leq 2.0$. We furthermore assume the position-dependent model of [1] for the observation noise covariance: $\mathrm{tr}\left\{\Phi^{-1}(q_{i,t}, p_t)\right\} = 1/g(\|q_{i,t} - p_t\|)$, where $g(r) = \varpi(r - r_s)^2 + \nu$, $\varpi > 0$ and $\nu > 0$ are scaling constants and r_s is the sweet spot radius, where the sensing quality is the best. For this example we use $\varpi = 0.008$, $\nu = 0.08$ and $r_s =$

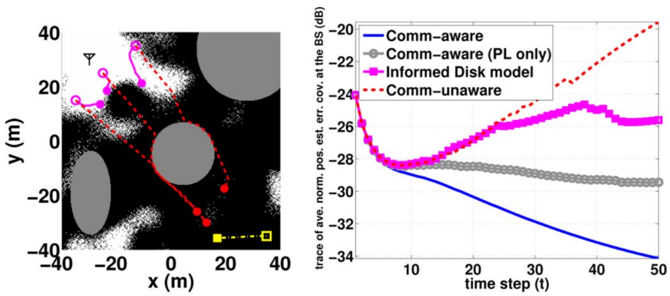

(a) (b)

Fig. 4. Performance of the proposed communication-aware target tracking framework in an outdoor environment— (a) The left figure shows the trajectories of the nodes and the target. The solid magenta and dashed red lines correspond to the trajectory of the nodes in communication-aware and communication-unaware cases, respectively, while the yellow dash-dot line represents the trajectory of the target. The empty circles/box and the filled ones show the initial and final positions of the robots/target, respectively. (b) The right figure compares the performance of four approaches, with different levels of communication-awareness, in terms estimation error covariance at the fixed station.

[4]In this part, our focus is on the cooperation between each node and the base station and we are not concerned with decision coordination or communication interference among the nodes.

[5]In practice, the receiver drops the packets based on the quality of decoding. In [13], it was shown that this is equivalent to having a received channel power threshold.

1.0 m. The outdoor channel is simulated using the following parameters: $\theta = [-10 \quad 2.0]^{\mathrm{T}}$, $\xi = 4.0$ dB, $\beta = 20$ m and $\omega = 1.13$ dB (corresponding to a Nakagami distribution with parameter $m = 15.75$). Furthermore, $\epsilon = 0.5$ s, $\Theta = 0.001 I_2$ and $\Upsilon_{\mathrm{dB,TH}} = -40$ dB. In order to compare the performance of our communication-aware framework with more traditional approaches, the figure shows four different cases: 1) **comm-aware**, 2) **comm-aware (PL-only)**, 3) **informed disk model** and 4) **comm-unaware**. Comm-aware case is the full communication-aware framework of (4). On the other hand, comm-aware (PL-only) is a simplified yet probabilistic version of our framework where the correlation of the shadowing part is not utilized. In this case, the average of the channel is estimated by considering only the path loss parameters in (4) ($\hat{\Upsilon}_{\mathrm{dB},i,t}(q) = \gamma^{\mathrm{T}}(q)\theta$ in Lemma 2) and the variance is calculated accordingly. As we shall see from our results, this approach is more suitable for the cases where the environment is multipath dominant (experiencing a small ratio of the correlated channel component to the uncorrelated part). Informed disk model is the case where each node models the link with a disk model (which is common in the robotics literature). However, it is a more informed approach, in which our channel assessment framework is utilized to assess the path loss decay rate. Then a disk is specified based on $\Upsilon_{\mathrm{dB,TH}}$. Finally, the comm-unaware case is the case where each node only considers its sensing objectives. Fig. 4(a) shows the trajectories of the nodes for comm-aware (solid magenta lines) and comm-unaware (dashed red lines) cases, superimposed on the connectivity map of the received channel power to the base station, with the white (black) regions denoting the connected (disconnected) areas. For better visualization, we did not include the trajectories of the other two cases. The performance of all the four cases is then compared in Fig. 4(b), where the trace of the average normalized error covariance of target position estimation at the base station (averaged over 30 runs) is plotted as a function of time. It can be seen that the communication-aware case performs considerably better than the other approaches as it maintains the connectivity of the nodes to the base station with high probability. This is then followed by the performance of the PL-only case, the informed disk model case and the unaware case, as expected. It can also be observed that the corresponding Kalman filter of the unaware case becomes unstable since the robot loses its connectivity after some steps. Note that in all the cases, each node solves for its corresponding next-step motion optimization problem locally, in a small area around it. Furthermore, in all the cases, the nodes start with 0.1% *a priori* randomly-positioned channel measurements in the environment (102 measurements for a 320×320 grid).

Fig. 5 compares the performance of the aforementioned four approaches in an indoor environment. In this case, the performance is simulated in a real environment in our building, in terms of channel measurements. The figure shows the blueprint of the basement of the Electrical and Computer Engineering building at the University of New Mexico, with the true connectivity map to the fixed station superimposed on it. Aside from the underlying channel, all the other parameters are the same as for Fig. 4, except that we only have one node with $\|v_{i,t}\| \leq 0.8$ and $\Upsilon_{\mathrm{dB,TH}} = -50$ dB. As can be seen, the aforementioned four approaches (averaged over 30 runs) compare similar to Fig. 4. In this case, however, the performance of comm-aware (PL only) case is very close to that of the comm-aware case since the ratio of the power of the correlated channel component to that of the uncorrelated part is lower ($\xi^2/\omega^2 = 1.13$ as compared to $\xi^2/\omega^2 = 13.22$ for Fig. 4) and the decorrelation distance is also smaller ($\beta = 0.32$ m as compared to $\beta = 20$ m for Fig. 4), as expected. Furthermore, the error of both comm-unaware and informed disk model cases increases since they cannot maintain proper connectivity. Overall, our results indicate that networked robotic operations can benefit considerably from our probabilistic channel assessment and its integration with sensing/motion planning.

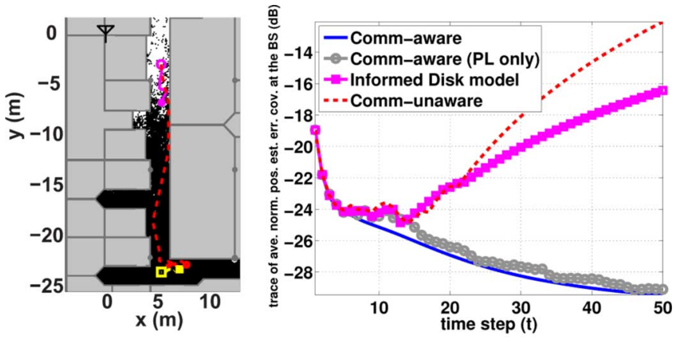

(a) (b)

Fig. 5. Performance of the proposed communication-aware target tracking framework in an indoor environment (basement of the Electrical and Computer Engineering building at the University of New Mexico)— (a) The left figure shows the trajectories of the node and the target (see the explanation of Fig. 4). (b) The right figure compares the performance of four approaches, with different levels of communication-awareness, in terms estimation error covariance at the fixed station.

IV. Conclusion

In this technical note, we proposed a communication-aware motion planning framework to increase the probability that a robot maintains its connectivity to a fixed station, while tracking a target in realistic communication environments. We used a probabilistic multi-scale model for channel characterization and presented a probabilistic framework for assessing the spatial variations of a wireless channel, based on a small number of measurements. We then showed how this channel learning framework can be utilized for devising communication-aware motion-planning strategies for 1) improving channel modeling and assessment and 2) communication-aware target tracking. For the latter, we showed how probabilistic channel assessment metrics can be combined with sensing goals, when controlling the motion, in order to increase the amount of information that the fixed station receives about the target. Finally, we showed the performance of our framework, using both real and simulated channel measurements.

References

[1] A. Ghaffarkhah and Y. Mostofi, “Channel learning and communication-aware motion planning in mobile networks,” in *Proc. Amer. Control Conf. (ACC)*, Jun. 2010, pp. 5413–5420.

[2] Y. Mostofi, M. Malmirchegini, and A. Ghaffarkhah, “Estimation of communication signal strength in robotic networks,” in *Proc. IEEE Int. Conf. Robot. Autom. (ICRA)*, May 2010, pp. 1946–1951.

[3] M. Ji and M. Egerstedt, “Distributed coordination control of multiagent systems while preserving connectedness,” *IEEE Trans. Robotics*, vol. 23, no. 4, pp. 693–703, Aug. 2007.

[4] C. Dixon and E. Frew, “Maintaining optimal communication chains in robotic sensor networks using mobility control,” *Mobile Netw. Appl.*, vol. 14, pp. 281–291, 2009.

[5] M. Lindhe and K. H. Johansson, “Using robot mobility to exploit multipath fading,” *IEEE Wireless Commun.*, vol. 16, no. 1, pp. 30–37, Feb. 2009.

[6] Y. Mostofi, “Decentralized communication-aware motion planning in mobile networks: An information-gain approach,” *J. Intell. Robot. Syst., Special Issue Unmanned Auton. Veh.*, vol. 56, pp. 233–256, 2009.

[7] A. Ghaffarkhah and Y. Mostofi, “Communication-aware navigation functions for cooperative target tracking,” in *Proc. Amer. Control Conf. (ACC)*, Jun. 2009, pp. 1316–1322.

[8] M. Malmirchegini and Y. Mostofi, “On the spatial predictability of communication channels,” *IEEE Trans. Wireless commun.*, submitted for publication.

[9] A. Goldsmith, *Wireless Communications*. Cambridge, U.K.: Cambridge Univ. Press, 2005.

[10] A. Ghaffarkhah and Y. Mostofi, “A foundation for communication-aware surveillance in mobile networks,” *IEEE Trans. Signal Processing*, submitted for publication.

[11] S. L. Cotton and W. G. Scanlon, "Higher order statistics for lognormal small-scale fading in mobile radio channels," *IEEE Antennas Wireless Propa. Lett.*, vol. 6, pp. 540–543, 2007.
[12] H. V. Poor, *An Introduction to Signal Detection and Estimation*, 2nd ed. Berlin, Germany: Springer-Verlag, 1994.
[13] D. Son, B. Krishnamachari, and J. Heidemann, "Experimental study of concurrent transmission in wireless sensor networks," in *Proc. 4th Intl. Conf. Embedded Networked Sensor Syst.*, 2006, pp. 237–250.
[14] K. V. Ramachandra, *Kalman Filtering Techniques for Radar Tracking*. New York: Marcel Dekker, 2000.

Distributed Task Assignment in Mobile Sensor Networks

Carlos H. Caicedo-Núñez and Miloš Žefran

***Abstract*—We study the task allocation problem: how a set of mobile agents can best monitor a convex region and at the same time localize events such as biochemical threats that appear in the region. As the agents move towards an event to localize it, the coverage of the region deteriorates; on the other hand, if an agent does not help in localizing an event, it will take longer for other agents to localize it. The decision on how an agent should trade off localization and coverage depends on a particular network deployment. We show how different deployments can be parametrized and propose a distributed algorithm to solve the task allocation problem. The algorithm is shown to be stable and scalable, and is shown to converge to an optimal equilibrium position. The proposed parametrization of the task allocation problem depends on the number of agents in the network; we thus present a fast and robust algorithm based on consensus protocols for estimating this number.**

***Index Terms*—Distributed control, distributed counting, robotic networks, task assignment.**

I. Introduction

Several authors have studied the problem of how agents in a mobile sensor network can be perform a given task. In [1], [2], the authors study how sensors can be moved to optimize the coverage of a convex region. Estimation of the location of a biochemical source with a sensor network is studied in [3], [4]. The consensus problem for sensor networks was studied in [5]–[9], among others.

However, there are few formal results for the case when the network needs to perform more than one task. Solutions that have been proposed are mainly empirical, rely on centralized algorithms, or focus on the case when several instances of a single task need to be performed. Distributed task assignment problem has been studied in [10]; for an extension to a probabilistic setting see [11] and the references therein. Similarly, [12] studies the multi-foraging task. In these works the focus is either on how to choose an agent to perform a task (respond to an event) using centralized algorithms, or on how to choose an instance of the same task based on local information. In [13], a time-varying density function is used to achieve simultaneous coverage and tracking. Market-based approaches to task allocation have been studied in [14]–[18]. However, a disadvantage of these techniques compared to fully distributed approaches is that when "fully distributed approaches exist, market approaches can be unnecessarily complex in design and have greater communication and computation requirements" [17]. On the other hand, compared to our approach, market-based approaches are more general and can deal with a variety of constraints.

We focus on the problem of how agents in a mobile network can respond to stationary events while maintaining sufficient coverage of the region. We present a fully distributed algorithm that addresses tasks which differ from each other and may require more than one agent to complete. A framework is proposed for formally specifying how different tasks should be handled by the network. Since this specification depends on the number of agents in the network, we also present a distributed algorithm that estimates this number.

Manuscript received April 02, 2010; revised April 15, 2010; accepted July 12, 2011. Date of publication August 08, 2011; date of current version October 05, 2011. This paper was presented in part at the IEEE Conference on Decision and Control, 2007. This work was supported by National Science Foundation (NSF) grants IIS-0905593, CNS-0910988 and CNS-1035914. Recommended by Associate Editor I. Stojmenovic.

C. H. Caicedo-Núñez is with the Department of Mechanical and Aerospace Engineering, Princeton University, Princeton, NJ 08544 USA (e-mail: ccaicedo@princeton.edu).

M. Žefran is with the Department of Electrical and Computer Engineering, University of Illinois at Chicago, Chicago, IL 60607 USA (e-mail: mzefran@uic.edu).

Color versions of one or more of the figures in this paper are available online at http://ieeexplore.ieee.org.

Digital Object Identifier 10.1109/TAC.2011.2164029

II. Model

Let $\mathcal{A} \subset \mathbb{R}^m$ be a bounded convex set. Consider n robotic agents, where $p_i \in \mathcal{A}$ is the position of agent i with respect to a universal frame (for instance, determined via GPS). Let $\mathcal{S}$ be an event located in $s \in \mathcal{A}$. Each agent possesses a sensor that at a distance d from the event returns the measurement $S_d = \mathfrak{F}(d) + \mathfrak{N}$, where $\mathfrak{F} : \mathbb{R} \to \mathbb{R}$ is a decreasing function of d and $\mathfrak{N}$ is the measurement noise. Our algorithm works for sensor models for which there exists a consistent estimator for d. For instance, a model inspired by chemical diffusion sources [3] is $S_d = K/(d^2+1) + \mathfrak{N}$, where K is a constant that we assume to be known (it is easy to extend the approach to also estimate K) and $\mathfrak{N}$ is Gaussian measurement noise with zero mean and variance σ^2.

Let $\|x\|$ be the euclidean norm of vector x, and $Q_i \subseteq \mathcal{A}$ be the Voronoi region [19] generated by the agent i, $Q_i = \{q \in \mathcal{A} : \|q - p_i\| \leq \|q - p_j\|, j \in \mathbb{N}, 1 \leq j \leq n\}$. Agents i and j are said to be *Voronoi neighbors* if $Q_i \cap Q_j \neq \emptyset$. In particular, an agent i is a neighbor of itself. We assume that i can determine the set of its Voronoi neighbors and that the agent i can communicate with every Voronoi neighbor j (implying that the communication graph is always connected). See [20] for details on distributed computation of Voronoi diagrams and [21] for generalizations to agents with limited sensing range.

There is no intrinsic way of determining relative importance of different tasks in a network, the assignment depends on a particular deployment of the network. In order to formally describe different scenarios we thus assume that the number of agents that need to be assigned to a particular event $\mathcal{S}$ is given by a function $\mathcal{P}_{\mathcal{S}} : \mathbb{N} \to \mathbb{N}$ that determines the number of agents that should be assigned to $\mathcal{S}$ given the number of deployed agents n. This function is typically determined when the network is deployed to tune it to a particular usage scenario and will be assumed to be known to the agents.

For each agent one of two possible states is defined: every agent i is either performing an *event-response* task (state 1) or performing *coverage* (state 2). We refer to the former agents as the *sensing* agents, while the latter agents are referred to as the *coverage* agents. Assume the sensor location evolves according to the first order dynamics in continuous time, $\dot{p}_i = u_i$, where u_i is the motion control input for state i. This paper studies the case when the sensor motion is governed by the following control laws $u_i = -k_1(p_i - s_i),\ k_1 > 0$ in state 1, and $u_i = -k_2(p_i - C_i),\ k_2 > 0$ in state 2, where s_i is the estimate of the event location s generated through a consistent estimator by agent i